Journal of Organometallic Chemistry, 391 (1990) 345–360
Elsevier Sequoia S.A., Lausanne
JOM 20887

Molecular structure, bonding, and reactions of $Mo(\eta^5\text{-}C_5H_5)_2$ derivatives containing phosphorus ligands. Crystal structures of $[Mo(\eta^5\text{-}C_5H_5)_2H(PPh_3)]I \cdot \frac{1}{2}H_2O$ and $[Mo(\eta^5\text{-}C_5H_5)_2(CH_3)(PPh_3)][PF_6]$

C.G. Azevedo, M.J. Calhorda, M.A.A.F. de C.T. Carrondo, A.R. Dias, V. Félix and C.C. Romão

Centro de Química Estrutural, Complexo I, Instituto Superior Técnico, 1096 Lisboa Codex (Portugal)

(Received January 9th, 1990)

Abstract

The oxidative addition reactions of $[Mo(\eta^5\text{-}C_5H_5)_2(PPh_3)]$, prepared by deprotonation of $[Mo(\eta^5\text{-}C_5H_5)_2H(PPh_3)][PF_6]$ with HCl, CH_3I, $(CH_3)_3SiCl$ and $(C_2H_5)_2S_2$ are described. Two of the complexes obtained have been characterized by single crystal X-ray diffraction studies, viz: $[Mo(\eta^2\text{-}C_5H_5)_2H(PPh_3)]I.1/2H_2O$ (**1a**) and $[Mo(\eta^5\text{-}C_5H_5)_2(CH_3)(PPh_3)][PF_6]$ (**3**). In complex **1a**, the Mo–H and Mo–P bond lengths are 1.74(8) and 2.501(4) Å, and the H–Mo–P angle is 77(2)°, while in complex **3** the Mo–C and Mo–P bond lengths are 2.269(7) and 2.526(4) Å and the C–Mo–P angle is 84.1(2)°.

Molecular orbital and steric energy calculations have been carried out for some model complexes in order to throw light on their geometrical preferences and to evaluate the influence of a bulky ligand in association with a small hydride on the overall geometry of the molecule.

Introduction

Deprotonation of bis(cyclopentadienyl)molybdenum or -tungsten hydride complexes containing a bond between the transition metal and a Main Group element such as P or Sn, e.g. $[M(Cp)_2H(SnR_2X)]$ ($Cp = \eta^5\text{-}C_5H_5$), has received considerable attention. The reactions lead to molybdenocene adducts, such as $Cp_2Mo{=}SnR_2$ or $Cp_2Mo{=}PAr$ [1]. Interestingly a structural study of $[Mo(Cp)_2H(SnR_2X)]$ complexes revealed considerable distortion of the normal $[Mo(Cp)_2LL']$ geometry [2]. We describe here another deprotonation reaction, which can generate a synthetically useful stabilized $Mo(Cp)_2$ fragment, namely the deprotonation of the cation $[Mo(Cp)_2H(PPh_3)]^+$. The structure of this cation in the hydrated iodide salt **1a** was

0022-328X/90/$03.50

determined, and revealed to have a high degree of distortion at the LMoL′ angle (L = H, L′ = PPh_3). Molecular orbital and steric energy calculations have been carried out in order to account for the experimental findings.

Results and discussion

Chemical studies

The salt $[Mo(Cp)_2H(PPh_3)][PF_6]$ (**1b**) can be readily prepared from $[Mo(Cp)_2H(I)]$ and PPh_3 in the presence of $Tl[PF_6]$ [3]. It seemed to us likely that deprotonation of **1b** would give $[Mo(Cp)_2(PPh_3)]$ (**2**), an exceedingly reactive molybdenocene derivative which was prepared previously by photochemical reaction of $[Mo(Cp)_2H_2]$ with PPh_3 in isooctane [4].

In order to examine this possibility a suspension of **1b** in toluene was treated with NaH at ca 50 °C. The resulting orange-brown solution was filtered and treated with gaseous HCl. A yellow precipitate separated instantaneously, and after work-up in aqueous NH_4PF_6 this was shown to be **1b** by ^1H NMR and IR spectroscopy. This result implies a reversible proton exchange at the metal as in eq. 1.

$$[Mo(Cp)_2H(PPh_3)]^+ \underset{HCl}{\overset{NaH}{\rightleftharpoons}} [Mo(Cp)_2(PPh_3)] \quad (1)$$

(1b) **(2)**

Attempts to isolate **2** from the toluene orange solution were frustrated by its progressive decomposition at room temperature and by the fact that free PPh_3 resulting from this decomposition co-sublimes with the product. We therefore decided to carry our studies on freshly prepared and filtered solutions of **2** formed in situ by NaH-deprotonation of **1b**.

Addition of CH_3I to a solution of **2** gave a precipitate, which was treated with aqueous $NH_4[PF_6]$ to give the known $[Mo(Cp)_2(CH_3)(PPh_3)][PF_6]$ (**3**) [5], which was characterized by ^1H NMR and IR spectroscopy and a single crystal X-ray diffraction structure determination (see below).

These results closely parallel those observed with the isoelectronic complex $[Mo(Cp)_2(C_2H_4)]$, which also undergoes reversible protonation at the metal and adds to CH_3I to give, after treatment with $NH_4[PF_6]$, the salt $[Mo(Cp)_2(CH_3)(C_2H_4)][PF_6]$ [5]. However, this type of nucleophilic addition of **2** to electrophiles is not always observed. Thus the reaction of **2** with C_2H_5I and $PhCH_2Br$ does not give salts of the corresponding $[Mo(Cp)_2R(PPh_3)]^+$ cations (R = C_2H_5, CH_2Ph). The only tractable products isolated were $[R(PPh_3)]^+$ salts, identified by ^1H NMR spectroscopy. Even more unexpected was the formation of $[Mo(Cp)_2H(PPh_3)]Cl$ (isolated in 40% yield) in the reaction of **2** with $(CH_3)_3SiCl$ followed by anhydrous work-up. We cannot account for this result in respect of the origin of the metal-bound hydrogen, and the reaction is being further investigated. It is conceivable that when steric effects hinder nucleophilic displacement, alternative reaction pathways are favoured. If, e.g., PPh_3 dissociation takes place, the resulting molybdenocene could give various products through oxidative additions and/or radical pathways. In fact, **2** reacts with $(C_2H_5)_2S_2$ at ca 50 °C to give $[Mo(Cp)_2(SC_2H_5)_2]$ in high yield [6]. The same product is formed in somewhat lower yield by reaction of $[Mo(Cp)_2(\eta^2\text{-}C_2H_2Ph_2)]$, a well known molybdenocene precursor [7], with $(C_2H_5)_2S_2$.

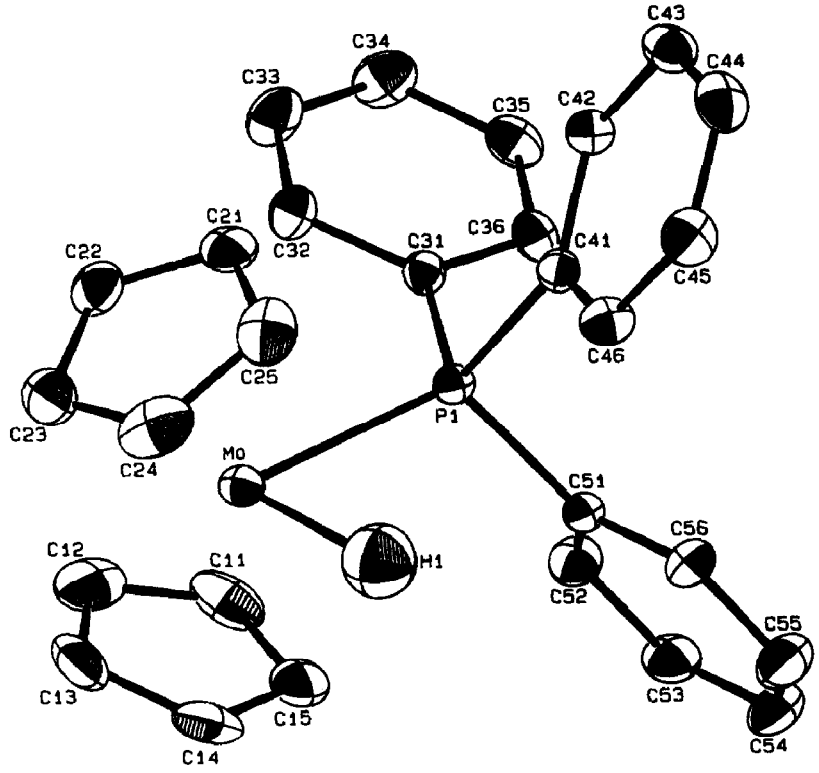

Fig. 1. Molecular structure of $[Mo(Cp)_2H(PPh_3)]^+$ in **1a**, with 30% thermal ellipsoids.

It thus seems that **2** is a readily available source of stabilized molybdenocene, and we are currently studying the addition of this species to other reactive single bonds, such as O–O, Se–Se, P–P, and Si–Si bonds.

Molecular structures of $[Mo(Cp)_2H(PPh_3)]I \cdot \frac{1}{2}H_2O$ *(1a) and* $[Mo(Cp)_2(CH_3)(PPh_3)][PF_6]$ *(3)*

The molecular structure of **1a** and **3** are shown in Figs. 1 and 2, respectively. Selected bond lengths and bond angles are given in Tables 1 and 2 for complexes **1a** and **3**, respectively.

The unit cell for **1a** contains four $[Mo(Cp)_2H(PPh_3)]^+$ cations, four I^- anions, and two water molecules. The metal atom is coordinated to two η^5-cyclopentadienyl rings, the phosphorus atom of the triphenylphosphine, and the hydrogen atom, in a distorted tetrahedral arrangement.

The unit cell for **3** (Fig. 2) contains four $[Mo(Cp)_2(CH_3)(PPh_3)]^+$ cations and four $[PF_6]^-$ anions. The environment of the molybdenum atom is similar to that in **1a**, with the hydride atom replaced by the methyl group.

Figs. 3 and 4 show molecular projections into the H/CH_3–Mo–P planes for the two cations. The planar Cp rings adopt an eclipsed orientation in complex **3**, with a 0.2(9)° angle of tilt between the plane defined by the ring normals and the equatorial plane. However, in complex **1a** the two Cp rings are not superimposed, leading to an angle of tilt of 3(2)°.

The bond angle H–Mo–P in complex **1a**, 77(2)°, is within the observed experimental range for complexes with two monodentate ligands [8] or those with no

Table 1

Selected bond lengths (Å) and angles (°) for $[Mo(Cp_2)H(PPh_3)]I.\ \frac{1}{2}H_2O$

Bond lengths			
P(1)–Mo	2.501(4)	H(1)–Mo	1.74(8)
C(11)–Mo	2.314(7)	C(21)–Mo	2.359(7)
C(12)–Mo	2.316(8)	C(22)–Mo	2.342(7)
C(13)–Mo	2.314(7)	C(23)–Mo	2.287(7)
C(14)–Mo	2.289(7)	C(24)–Mo	2.265(7)
C(15)–Mo	2.266(7)	C(25)–Mo	2.307(7)
C(31)–P(1)	1.821(6)	C(41)–P(1)	1.839(6)
C(51)–P(1)	1.843(6)		
Cp rings		*Phenyl rings*	
C–C range	1.37(1)	C–C range	1.377(8)
	1.42(1)		1.410(7)
Bond angles			
H(1)–Mo–P(1)	77(2)	C(51)–P(1)–Mo	116.2(2)
C(31)–P(1)–Mo	116.6(2)	C(41)–P(1)–Mo	113.9(2)
C(41)–P(1)–C(31)	102.2(3)	C(51)–P(1)–C(31)	102.8(3)
C(51)–P(1)–C(41)	103.1(3)	C(32)–C(31)–P(1)	120.5(4)
C(46)–C(41)–P(1)	120.0(4)	C(52)–C(51)–P(1)	120.0(4)
C(56)–C(51)–P(1)	121.6(4)	C(36)–C(31)–P(1)	120.9(4)
C(42)–C(41)–P(1)	121.4(4)		
Cp rings		*Phenyl rings*	
C–C–C range	105.9(6)	C–C–C range	118.4(5)
	109.2(6)		121.0(6)

strain in chelating ligands [9]. The C–Mo–P angle of 84.2(1)° in complex **3** is at the long end of that range, possibly to minimize steric interactions between the methyl and the triphenylphosphine groups.

The Mo–P bond lengths in both complexes, 2.501(4) (**1a**) and 2.526(4) Å (**3**), are similar to those in $[Mo(Cp)_2(P_2H_4)]$ [10], 2.536(5) and 2.550(4) Å, but slightly longer than those in $[Mo(Cp)(\eta^3\text{-}C_5H_7)\{P(Ph_2)CH_2\}_2]$, 2.462(4) and 2.421(4) Å [11], or $[Mo(Cp)_2CH(CF_3)CH(CF_3)PPh_2]Cl \cdot H_2O$, 2.487(1) Å [12].

The mean bond lengths and bond angles in the complexed triphenylphosphines are identical with the values for free triphenylphosphine [13].

Table 3 lists relevant structural parameters for $[Mo(Cp)_2LL']$ complexes, in which L and L′ are the same or different. The length of the Mo–H bond in complex **1a** is similar to that determined by neutron diffraction for $[Mo(Cp)_2H_2]$ [14].

Discussion of other geometrical features is helped by use of another parameter, the angle between the M–L or M–L′ bond and line *z*, as defined by Bulychev et al. [2,16]. Line *z*, given by the intersection between the coordination plane, L,Mo,L′ and the plane of the ring normals, is useful for checking the degree of asymmetry observed in the complexes. This is more clearly seen in **a**.

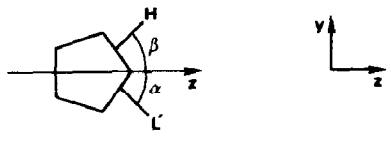

(a)

Table 2

Selected bond lengths (A) and angles (°) for $[MoCp_2(CH_3)(PPh_3)][PF_6]$

Bond lengths			
P(1)–Mo	2.526(4)	C(1)–Mo	2.269(7)
C(11)–Mo	2.315(8)	C(21)–Mo	2.330(7)
C(12)–Mo	2.330(8)	C(22)–Mo	2.360(8)
C(13)–Mo	2.335(8)	C(23)–Mo	2.327(7)
C(14)–Mo	2.321(7)	C(24)–Mo	2.282(7)
C(15)–Mo	2.288(7)	C(25)–Mo	2.271(7)
C(31)–P(1)	1.838(6)	C(41)–P(1)	1.841(6)
C(51)–P(1)	1.842(6)		
P–F range	1.538(6)		
	1.592(6)		
Cp rings		*Phenyl rings*	
C–C range	1.37(1)	C–C range	1.361(9)
	1.42(1)		1.403(7)
Bond angles			
C(1)–Mo–P(1)	84.1(2)		
C(31)–P(1)–Mo	116.1(2)	C(41)–P(1)–Mo	115.6(2)
C(51)–P(1)–Mo	115.5(2)	C(51)–P(1)–C(41)	105.1(3)
C(41)–P(1)–C(31)	100.2(3)	C(42)–C(41)–P(1)	120.4(4)
C(51)–P(1)–C(31)	102.2(3)	C(46)–C(41)–P(1)	121.8(4)
C(32)–C(31)–P(1)	120.8(4)	C(52)–C(51)–P(1)	119.6(4)
C(36)–C(31)–P(1)	120.2(4)	C(56)–C(51)–P(1)	121.8(4)
Cp rings		*Phenyl rings*	
C–C–C range	106.8(6)	C–C–C range	117.8(5)
	109.9(6)		121.6(5)

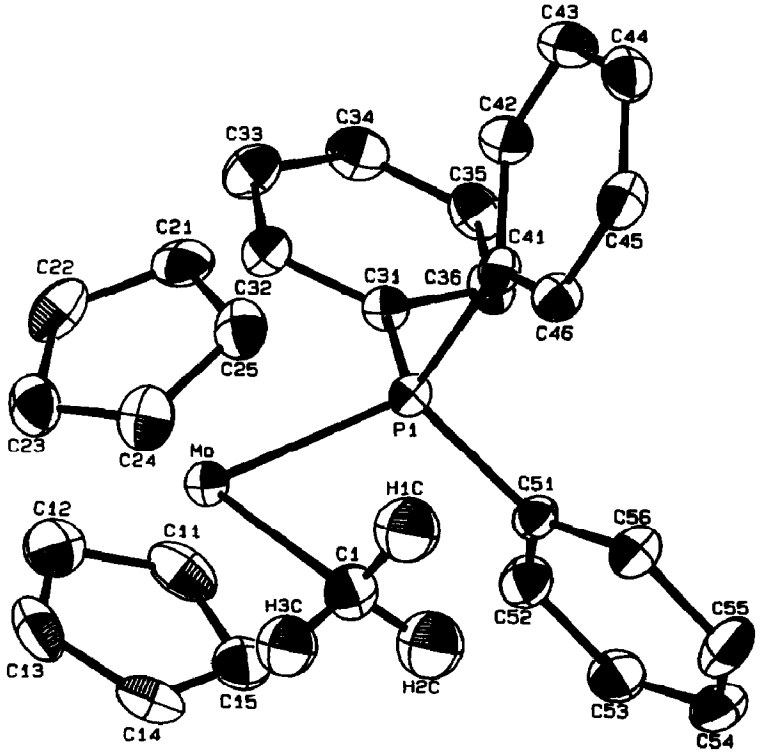

Fig. 2. Molecular structure of $[Mo(Cp)_2(CH_3)(PPh_3)]^+$ in 3, with 30% thermal ellipsoids.

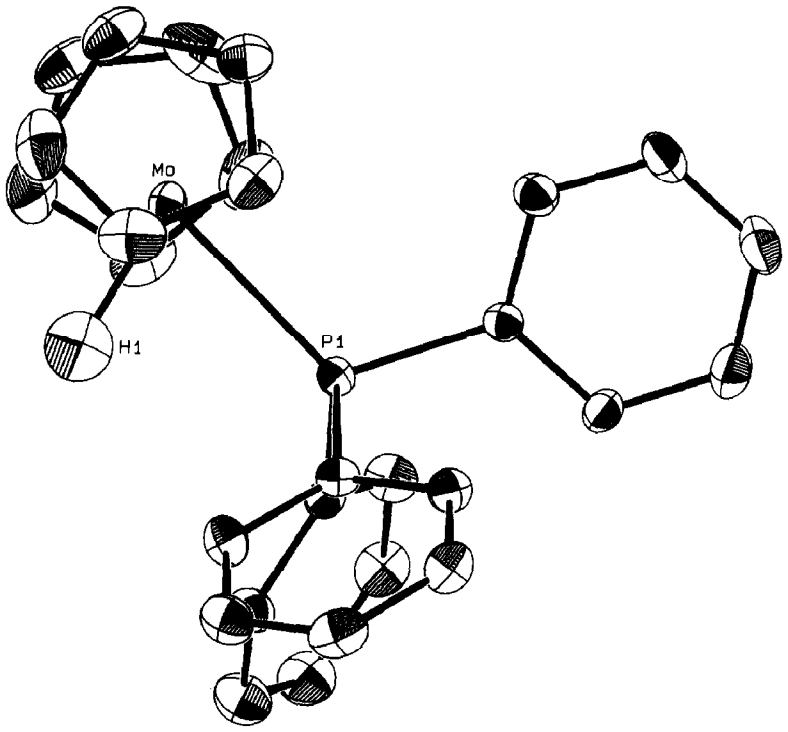

Fig. 3. Projection of the molecular structure of $[Mo(Cp)_2H(PPh_3)]^+$ in **1a** onto the H,Mo,P plane.

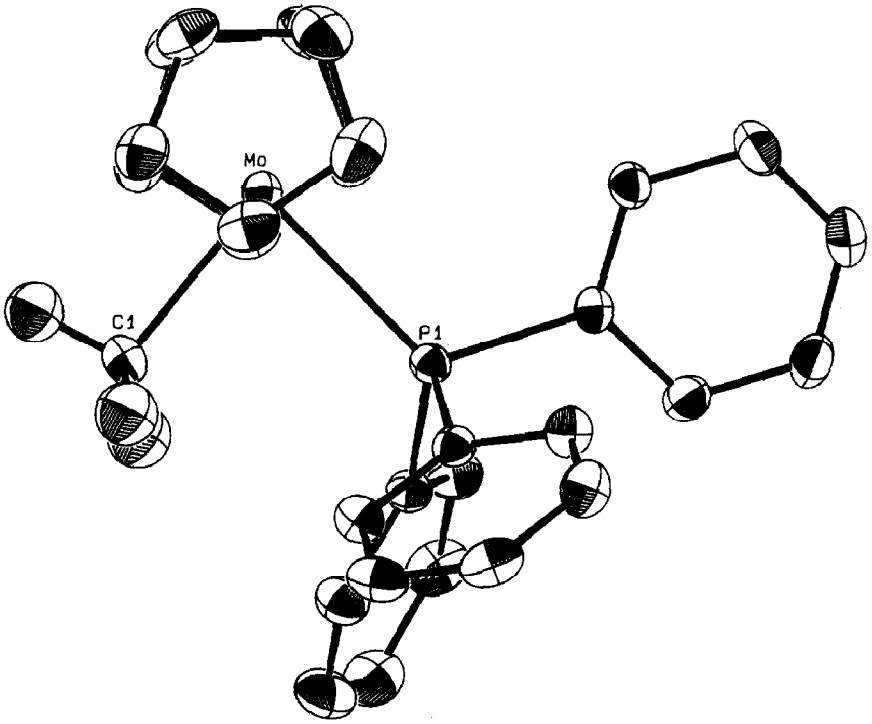

Fig. 4. Projection of the molecular structure of $[Mo(Cp)_2(CH_3)(PPh_3)]^+$ in **3** on to the C,Mo,P plane.

Table 3

Structural parameters for complexes $[Mo(Cp)_2LL']$

	Mo–H (Å)	Mo–C (Å)	LMoL′ (°)	Mo–Cp[a] (Å)	CpMoCp[b] (°)	zMoL(β) (°)	zMoL(α) (°)	Ref.
$[Mo(Cp)_2H(PPh_3)]I\cdot\frac{1}{2}H_2O$	1.74(8)		77(2)	1.973(1)	138.9(2)	54.(3)	23(1)	d
$[Mo(Cp)_2(CH_3)(PPh_3)][PF_6]$		2.269(7)	84.1(2)	1.985(1)	138.8(2)	51.7(1)	32.4(1)	d
$[Mo(Cp)_2H(SnMe_2Cl)]$	1.64(4)		72.7(2)	1.955	141.9	43.9	28.8	2
$[Mo(Cp)_2H(SnMe_3)]$[c]	1.60(5)		67.6(3)	1.952	141.9	38.5	29.1	2
	1.51(6)		69.5(3)	1.955	143.0	39.6	29.9	2
$[Mo(Cp)_2H_2]$	1.685(3)		75.5(3)	1.944(2)	145.8	37.75	37.75	14
$[Mo(Cp)_2(Bu)_2]$		2.270(3)	76.7(1)	1.974(3)	135.2(1)	38.35	38.35	15
$[Mo(Cp)_2H(SnCl_3)]$	1.74(7)		79(2)	1.962	141.3	53.2	26.0	16
$[Mo(Cp)_2(CHMeCN)(SPh)$		2.306(3)	77.4(1)	1.984	132.9	40.7	36.7	17
$[Mo(Cp)_2(NH_3)(SPh)][PF_6]\cdot Me_2Co$			76.4(4)	1.99(2)	134.9(7)	45.1	31.3	18

[a] Average ring normals. [b] Angle between the ring normals. [c] This complex contains two independent molecules by asymmetric unit. [d] This work.

When both ligands are the same as in $[Mo(Cp)_2H_2]$ and $[Mo(Cp)_2(Bu)_2]$, there is necessarily no asymmetry, and the angles, α and β, defined by this line are identical. However, when a bulky ligand is associated with a hydride in the coordination sphere, the asymmetry is substantial, with $\beta \gg \alpha$. This can be clearly seen from Fig. 3 for the cation $[Mo(Cp)_2H(PPh_3)]^+$, and a similar situation has been described for monohydride molybdenocene derivatives containing $SnCl_3$, $SnMe_2Cl$, and $SnMe_3$ as the L′ ligand (Table 3).

When the hydride is replaced by the bulkier methyl ligand, to give complex **3**, the asymmetry is not so marked, although still significant (Fig. 4). Similar small effects have been observed for other $Mo(Cp)_2$ derivatives containing ligands of different bulk, viz NH_3 with SPh, and $CH(CH_3)CN$ with SPh, as can be seen from Table 3.

It can be seen from figs. 3 and 4 that in both $[Mo(Cp)_2H(PPh_3)]^+$ and $[Mo(Cp)_2(CH_3)(PPh_3)]^+$ the small ligand, H or CH_3, is *trans* to one of the three phenyl groups of the phosphine ligand, the H or C atom being almost coplanar with the molybdenum and the phosphorus atom, as depicted in **b**.

This relative orientation of the ligands has been observed in other complexes, namely most of the tin derivatives (Table 3) and also $[Mo(Cp)_2(H)(SnBr_3)]$ [19] and $[Zr(Cp)_2Cl(SiPh_3)]$ [20], except that in complex $[Mo(Cp)_2(H)(SnCl_3)]$ [16] the relative orientation of the ligands is *cis*, as depicted in **c**.

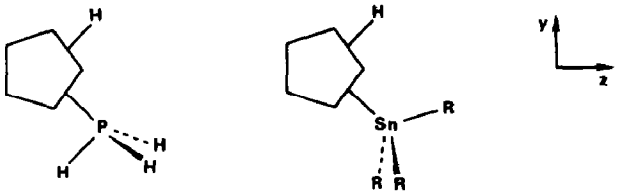

(b,trans) (c,cis)

Calculations

It was suggested previously [2] that the observed asymmetry in the $Mo(Cp)_2$ tin derivatives might be due to the special electronic characteristics of pyramidal tin(IV) bound to the hydride molybdenocene fragment. This structural feature was, however, observed for the hydridotriphenylphosphine species, and the distortion shown to be relieved when the small hydride ligand was replaced by the bulkier methyl.

Extended Hückel molecular orbital calculations [21] were performed on the model compounds, $[Mo(Cp)_2H(PH_3)]^+$ and $[Mo(Cp)_2H(SnCl_3)]$ in order to understand bonding in these complexes and look for any electronic effects that might be responsible for the distortion observed in the actual compounds.

The geometrical parameters to be considered are these shown above in **a**, **b** and **c**.

A projection of the molecule on the *yz* plane is given, and shows the angles α and β which define the position and asymmetry of the ligands relative to the *z* axis. Two conformations are possible for the PH_3 or $SnCl_3$ group (*trans*, **b** and *cis*, **c**), as mentioned before.

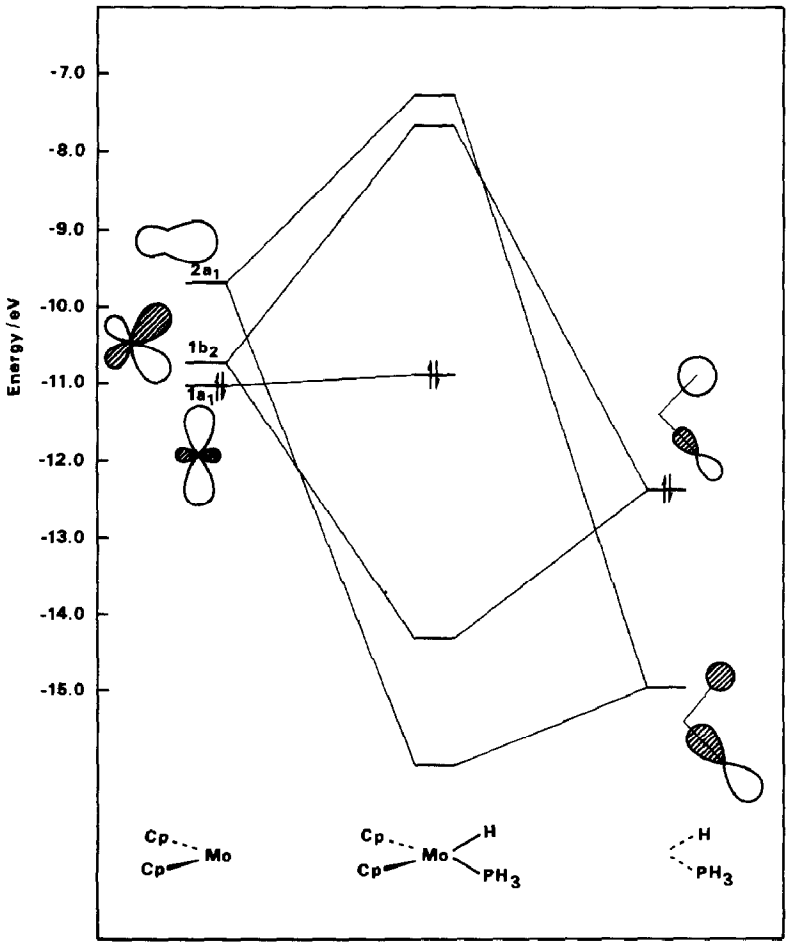

Fig. 5. Interaction diagram between the $Mo(Cp)_2$ fragment and the two ligands H and PH_3.

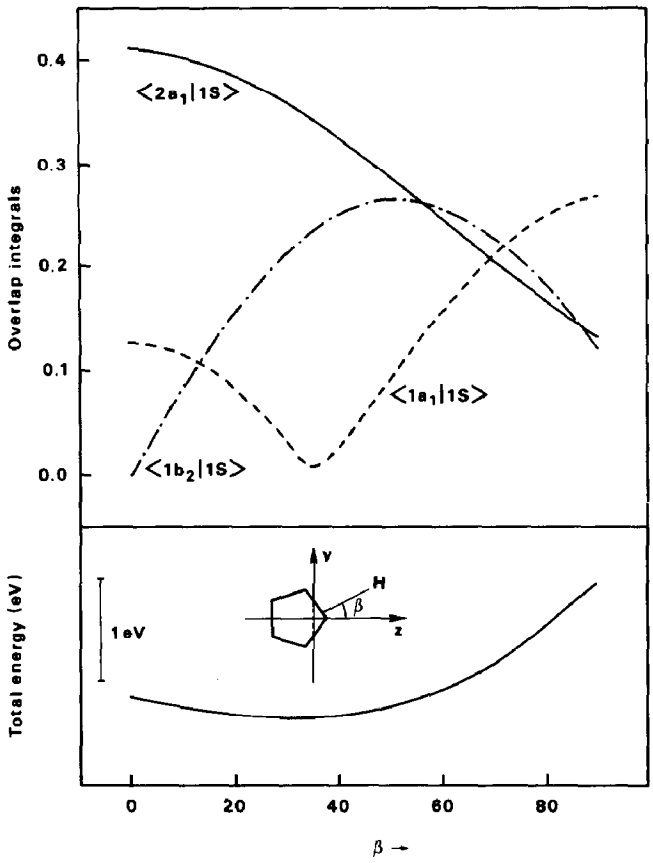

Fig. 6. Change in total energy and overlap integrals between the 1s hydrogen orbital and frontier orbitals of $Mo(Cp)_2$ as a function of the angle β.

For conformation **b**, α and β were varied for $[Mo(Cp)_2H(PH_3)]^+$ from a maximum $\alpha + \beta$ 90 to a minimum of 60°, both symmetrically ($\alpha = \beta$) and asymmetrically ($\beta > \alpha$). The lowest energy was found at β 55, α 27.5°, very close to the experimental geometry. It should be noted, however, that the energy for the symmetric geometry at $\alpha = \beta = 40°$ is only 0.14 eV higher, and the potential energy surface is soft (changing one angle by ca. 15°, typically induces a variation in energy of only about 0.1 eV).

These results suggest that there is no clear cut electronic preference for either structure. A molecular orbital interaction diagram for $[Mo(Cp)_2H(PH_3)]^+$ is shown in Fig. 5, for the experimental geometry (β 54, α 23°), and is similar to that normally expected for bent metallocene derivatives coordinated to σ donor ligands.

The symmetric and antisymmetric combinations of hydrogen 1s orbital and a mostly *p* orbital of tin donate electrons to empty b_2 and $2a_1$ $Mo(Cp)_2$ orbitals [8], $1a_1$ remaining almost non-bonding. The behaviour of the $[Mo(Cp)_2H]^+$ fragment illustrates what is happening. Fig. 6 shows how its energy changes as a function of the angle to the *z* axis (which corresponds to the experimentally defined *z* line).

The change is very smooth, at least up to ca. 60° (remember the experimental angle 54°) and the reason is, as can be seen from Fig. 6b, that although overlap

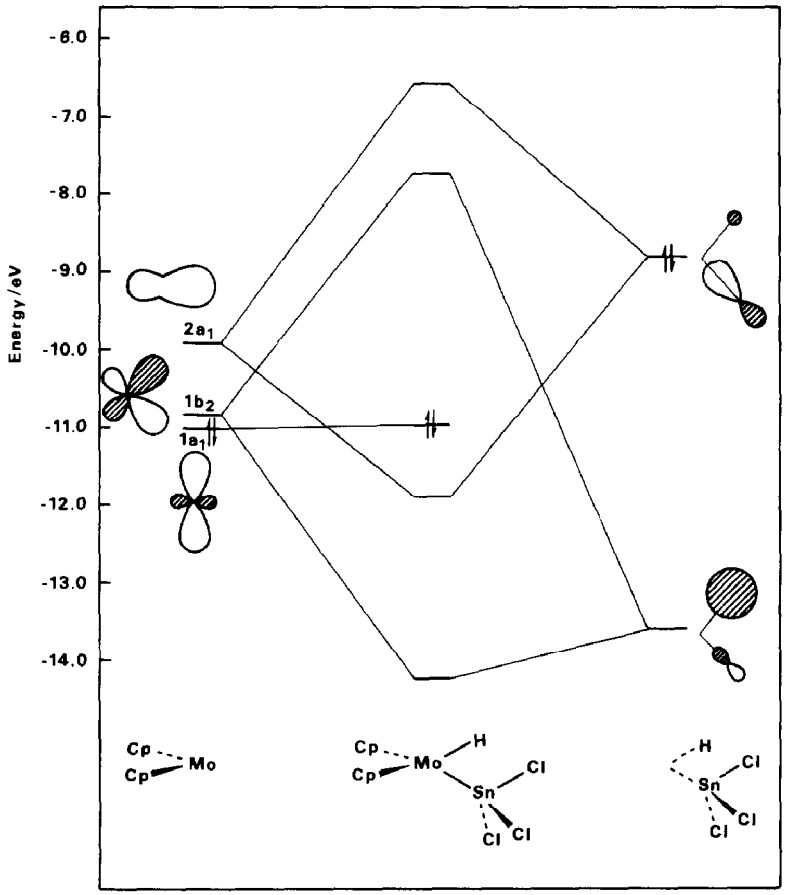

Fig. 7. Interaction diagram between the $Mo(Cp)_2$ fragment and the ligands H and $SnCl_3$.

between $2a_1$ and $1s$ is lost as the angle increases, it is compensated by a much better overlap with b_2, and for some positions with $1a_1$.

This means that the electronic requirements of the $Mo(Cp)_2$ fragment are not very strict, and a wide range of ligand angles can be accommodated around the metal atom, as was noted previously for the case of bidentate ligands forming four membered metallocycles [9]. The interaction of $Mo(Cp)_2$ with a hydride and $SnCl_3$ is shown in Fig. 7, and is similar to that observed for hydride and PH_3, suggesting that our results qualitatively hold also for the family of tin derivatives.

Having established that the electronic factors are not dominant (the same conclusion holds out for the tin derivatives) in determining the geometry of these hydride complexes, steric energy calculations using the EENY2 program [22] were made for the real $[Mo(Cp)_2H(PPh_3)]^+$ cation taking account of the actual bulk of the ligands.

In the first set of calculations the relative orientation of the phosphine ligand was allowed to change by rotating around the Mo–P bond (H–Mo–P–C torsion angle) and optimizing the relative orientation of the three phenyl rings (torsion angles Mo–P–C–C) for each position. The *trans* conformation, **b**, was found to be more stable than the *cis* geometry, as in **c**, by about 21 kcal mol^{-1}. Interactions between

hydrogens of the phenyl rings with those of Cp rings in the *cis* forms are responsible for this difference.

Extended Hückel calculations on the model PH_3 derivative also show the *trans* form to be more stable, although by only ca. 4 kcal mol^{-1}.

In the second set of calculations, the angles α and β were allowed to change from their actual values towards a symmetrical situation, with $\alpha + \beta$ kept fixed. This is allowable since it was shown earlier that the energy changes are only slightly affected by electronic factors. The energy increases by 293 kcal mol^{-1} if the rest of the molecule is kept fixed. Alternatively, if the geometry is allowed to relax the optimized values for these two angles are found to be 58 and 15°, respectively.

Another specific question involves the preference for a *trans* or *cis* conformation (**b** and **c**, see above) of the ligands, since we know that either can be adopted. We found that the energies were very similar for a series of derivatives (L = H, L' = PH_3, $SnCl_3$, $SnHCl_2$, SnH_2Cl, SnH_3), making it impossible to trace the origin of the preference. From what has been said above, we believe it to be steric, the delicate interplay of the several types of repulsions (L–L',Cp–L,Cp–L',Cp–Cp) leading to different conformations. Some of these effects have been discussed previously [23]. We did not find any evidence for the previously suggested [16] hydrogen bonding between the hydride and a chloride of $SnCl_3$ in $[Mo(Cp)_2H(SnCl_3)]$, which is known to adopt the *cis* conformation. The overlap population is close to zero and negative.

Experimental

Syntheses

General procedures

All reactions were performed under argon by standard Schlenk techniques. Toluene and diethyl ether were dried over Na/benzophenone and CH_2Cl_2 over CaH_2. All were distilled and stored under argon. $[Mo(Cp)_2H(PPh_3)][PF_6]$ [3] and $[Mo(Cp)_2(\eta^2\text{-}C_2H_2Ph_2)]$ [7] were prepared by published procedures. All the other reagents were commercially available and used as received.

Preparation of [Mo(Cp)$_2$(PPh$_3$)] (2). In a typical preparation of this complex, $[Mo(Cp)_2H(PPh_3)][PF_6]$ (0.175 g; 0.303 mmol) was suspended in toluene (30ml) and a large excess (ca. 0.3 g) of NaH added. The mixture was kept at 50 °C with stirring for ca. 2 h, then the orange brown solution was filtered and used immediately without further treatment.

Reaction of [Mo(Cp)$_2$(PPh$_3$)] with HCl. When gaseous HCl was bubbled through a freshly prepared toluene solution of $[Mo(Cp)_2(PPh_3)]$, a yellow precipitate separated and the solution became colourless. The precipitate was filtered off and washed with Et_2O (3 × 5 ml), then taken up in H_2O and treated with aqueous $NH_4[PF_6]$. The resulting precipitate was filtered off, washed with a little water, dried, and recrystallized from CH_2Cl_2/Et_2O to give $[Mo(Cp)_2H(PPh_3)][PF_6]$ in 80% isolated yield.

Reaction of [Mo(Cp)$_2$(PPh$_3$)] with CH$_3$I. Addition of CH_3I (3 ml) to a freshly prepared solution of $[Mo(Cp)_2(PPh_3)]$ caused immediate precipitation of a yellow solid. This was filtered off, washed with Et_2O (2 × 3 ml), and taken up in 30 ml of a 3 : 1 *v/v* mixture of Me_2CO/H_2O and treated with aqueous $NH_4[PF_6]$. Evaporation

of the acetone gave a yellow solid, which was washed with water then recrystallized from acetone/H_2O to give orange crystals of $[Mo(Cp)_2(CH_3)(PPh_3)][PF_6]$ in 80% yield.

Reaction of $[Mo(Cp)_2(PPh_3)]$ with $(CH_3)_3SiCl$. $(CH_3)_3SiCl$ (3 ml) was added to a freshly prepared solution of $[Mo(Cp)_2(PPh_3)]$ in toluene. The precipitate was filtered off, and washed with toluene (2 × 5 ml) and Et_2O (2 × 5 ml). Recrystallization from CH_2Cl_2/Et_2O gave orange yellow crystals of $[Mo(Cp)_2H(PPh_3)]Cl$ in 40% yield.

Reaction of $[Mo(Cp)_2(PPh_3)]$ with Et_2S_2. Treatment of a freshly prepared toluene solution of $[Mo(Cp)_2(PPh_3)]$ with Et_2S_2 (3 ml) for 3 h gave an orange solution. This was evaporated to dryness and the orange residue washed with Et_2O (3 × 5 ml) and shown to be $[Mo(Cp)_2(SEt)_2]$ (95% yield) by comparison of its IR and ^1H NMR spectra with those of an authentic sample [6].

Reaction of $[Mo(Cp)_2(C_2H_2Ph_2)]$ with Et_2S_2. To a toluene solution (30 ml) of $[Mo(Cp)_2(C_2H_2Ph_2)]$ (0.120 g, 0.295 mmol) was added Et_2S_2 (3 ml), and the mixture kept at room temperature overnight. The volatile materials were evaporated off and the residue extracted with Et_2O to give an orange solution of unchanged $[Mo(Cp)_2(C_2H_2Ph_2)]$ and leave an orange residue of $[Mo(Cp)_2(SEt)_2]$ in 80% yield.

Table 4

Crystallographic data and Enraf–Nonius CAD-4 data collection parameters

Complex	**1a**	**3**
Formula	$[MoCp_2(H)(PPh_3)]I \cdot \frac{1}{2}H_2O$	$[MoCp_2(CH_3)(PPh_3)][PF_6]$
Space group	$P2_1/c$	$P2_1/c$
M_r	625.3	648.4
a, Å	14.581(3)	14.140(4)
b, Å	12.157(3)	12.529(1)
c, Å	15.615(4)	15.135(4)
β, deg	114.58(2)	94.71(1)
V, Å^3	2517.1	2672.4
Z	4	4
D_{calc} g/cm^3	1.65	1.61
Radiation	Mo-K_α (λ 0.71069)	Mo-K_α (λ 0.71069)
μ(Mo-K$_\alpha$), cm^{-1}	16.78	5.88
Scan type	$\omega-2\theta$	$\omega-2\theta$
Scan width (ω), deg	0.80 + 0.35 tan θ	0.80 + 0.35 tan θ
Maximum time, s	60	90
Collect range	$\pm h, -k, -l$; $3.0 < 2\theta < 50°$	$\pm h, +k, +l$; $3.0 < 2\theta < 56°$
No. of data collected	4848	6936
No. of unique data	4153	5409
No of data $F > 3\sigma(F)$	3730	4203
Decay during collection	none	none
Data to parameter ratio	10.21	9.53
Largest shift/error on Final cycle		
Largest peak in final Difference Fourier, e/Å^3	0.20 1.29	0.15 0.75
R [a]	0.038	0.044
R_w [b]	0.045	0.042

[a] $R = \Sigma(|F_o| - |F_c|)/\Sigma|F_o|$. [b] $R_w = [\Sigma w(|F_o| - |F_c|)^2/\Sigma w|F_o|^2]^{1/2}$.

X-ray data collection, structure determination and refinement

The pertinent crystallographic parameters for complexes **1a** and **3** are given in Table 4.

The unit cell and orientation matrix were obtained in each case by least squares refinement from 25 centered reflections with $10 < \theta < 17°$ and $14 < \theta < 20°$ for **1a** and **3**, respectively. Intensity data were collected at room temperature on an Enraf–Nonius CAD-4 diffractometer with graphite monochromated Mo-K_α radiation, using a ω–2θ scan mode. The data were corrected for absorption, Lorentz and polarization effects with CAD-4 software.

Solution and refinement of the structures were carried out with the programme SHELX76 [24]. The ORTEPII programme [25] was used to draw the structures. The atomic scattering factors and anomalous scattering terms were taken from International Tables [26].

The Laue symmetry and systematic absences observed for both compounds are consistent with space group $P2_1/c$.

Table 5

Selected fractional atomic coordinates ($\times 10^4$) for $[Mo(Cp)_2H(PPh_3)]I \cdot \frac{1}{2}H_2O$

	x	y	z	U_{eq}
Mo	−1264.8(3)	3135.4(3)	−212.7(2)	30.2(2)
I	2097.4(3)	991.0(3)	28.9(3)	54.2(2)
H(1)	−110(5)	453(6)	−36(5)	9(2)
P(1)	−2808(1)	4001(1)	−184(1)	27(4)
C(11)	−2452(5)	2482(6)	−1633(4)	64(2)
C(12)	−1663(7)	1703(5)	−1285(4)	78(3)
C(13)	−793(5)	2206(6)	−1259(4)	61(2)
C(14)	−1015(5)	3274(6)	−1562(4)	62(3)
C(15)	−2040(5)	3450(6)	−1783(4)	59(2)
C(21)	−979(4)	2893(5)	1377(3)	48(2)
C(22)	−775(4)	1906(4)	1055(4)	48(2)
C(23)	32(4)	2077(5)	796(4)	58(3)
C(24)	318(4)	3204(6)	947(4)	65(2)
C(25)	−328(4)	3696(5)	1317(4)	60(2)
C(31)	−3749(3)	3071(3)	−105(3)	30(2)
C(32)	−3491(4)	1994(4)	212(3)	38(2)
C(33)	−4175(4)	1331(4)	363(4)	51(2)
C(34)	−5122(4)	1714(5)	197(4)	53(2)
C(35)	−5417(4)	2760(5)	−156(4)	46(2)
C(36)	−4729(3)	3446(4)	−291(3)	36(2)
C(41)	−2548(3)	4920(3)	826(3)	31(1)
C(42)	−3016(3)	4765(4)	1443(3)	36(2)
C(43)	−2818(4)	5476(4)	2190(3)	43(2)
C(44)	−2171(4)	6354(5)	2329(4)	50(2)
C(45)	−1691(4)	6510(4)	1740(4)	47(2)
C(46)	−1872(4)	5793(4)	994(3)	39(2)
C(51)	−3557(3)	4872(3)	−1202(3)	30(1)
C(52)	−4344(4)	4416(4)	−1978(3)	42(2)
C(53)	−4906(4)	5062(5)	−2757(3)	49(2)
C(54)	−4683(4)	6165(5)	−2775(4)	56(2)
C(55)	−3908(4)	6619(5)	−2006(4)	56(2)
C(56)	−3349(4)	5986(4)	−1223(4)	40(2)

The structures were solved by a combination of Patterson and difference Fourier methods. The refinement was carried out by full matrix least-squares for **1a** and bloc matrix least-squares for **3**. Some cycles with isotropic temperatures factors for nonhydrogen atoms gave $R = 0.093$ for **1a** and $R = 0.087$ for **3**. Anisotropic refinement reduced R to 0.050 and 0.054 for **1a** and **3**, respectively. After that refinement a Fourier difference map for **1a** showed an isolated peak with electron density of 2.583 $e\text{Å}^{-3}$, which was considered to be an oxygen atom of a water molecule with half occupancy. When this position was included and refined isotropically the R factor was reduced to 0.044.

Table 6

Selected fractional atomic coordinates ($\times 10^4$) for $[Mo(Cp)_2(CH_3)(PPh_3)][PF_6]$

	x	y	z	U_{eq}
Mo	3653.0(2)	1367.2(3)	1939.0(2)	33.2(1)
P(1)	2110(1)	754(1)	1139(1)	32.1(3)
C(1)	3798(4)	−368(4)	2357(4)	52(2)
C(11)	2588(4)	2329(5)	2707(3)	63(2)
C912)	3425(5)	2953(4)	2697(4)	71(2)
C(13)	4146(4)	2389(5)	3182(4)	66(2)
C(14)	3796(4)	1445(5)	3476(3)	63(2)
C(15)	2822(4)	1394(5)	3174(3)	58(2)
C(21)	3972(3)	1713(5)	480(3)	59(2)
C(22)	4422(4)	2503(5)	981(4)	64(2)
C(23)	5116(3)	2011(5)	1576(4)	59(2)
C(24)	5081(3)	915(5)	1443(4)	57(2)
C(25)	4360(3)	717(4)	757(4)	54(2)
C(31)	1294(3)	1812(3)	715(3)	35(1)
C(32)	1627(3)	2815(3)	533(3)	41(1)
C(33)	1030(3)	3582(4)	110(3)	52(2)
C(34)	91(4)	3325(4)	−100(3)	54(2)
C(35)	−264(3)	2348(4)	93(3)	51(2)
C(36)	335(3)	1579(4)	488(3)	44(1)
C(41)	2221(3)	−13(3)	115(3)	35(1)
C(42)	1887(3)	412(4)	−711(3)	46(1)
C(43)	2001(3)	−139(4)	−1478(3)	53(2)
C(44)	2429(4)	−1119(4)	−1457(3)	55(2)
C(45)	2767(3)	−1561(4)	−653(3)	52(2)
C(46)	2677(3)	−998(4)	123(3)	43(1)
C(51)	1347(3)	−65(3)	1799(3)	38(1)
C(52)	717(3)	432(4)	2326(3)	51(2)
C(53)	150(4)	−163(5)	2845(3)	60(2)
C(54)	204(4)	−1268(5)	2846(3)	66(2)
C(55)	834(4)	−1759(5)	2347(4)	66(2)
C(56)	1413(3)	−1166(4)	1820(3)	51(2)
P(2)	3190(1)	5760(1)	875(1)	54.0(4)
F(1)	3928(3)	6330(4)	351(3)	128(2)
F(2)	3975(3)	5314(4)	1548(4)	154(2)
F(3)	2433(3)	5179(3)	1432(3)	115(2)
F(4)	2379(3)	6186(4)	222(4)	146(2)
F(5)	3153(4)	6785(3)	1453(4)	163(3)
F(6)	3190(3)	4703(3)	323(3)	116(2)

In both structures hydrogen atoms were located from difference maps and refined isotropically, except for one hydrogen of one cyclopentadienyl of complex **1a**, which was included in the calculated position. The hydrogen atoms of the Cp and phenyl rings were refined in five different groups with the same U_{iso}. The distances C–H were fixed at 1.08 Å with routine DFIX of SHELX76. Two strong reflections (−221 and 121 for **1a**; 200 and −102 for **3**) thought to be affected by extinction were removed from the data. The weighting scheme $w = k/[\sigma^2(F_o) + g(F_o)^2]$ was applied with the refined values of $k = 1.0913$ and $g = 0.00213$ for **1a** and $k = 1.7749$ and $g = 0.00043$ for **3**. The final refinements converged at $R = 0.038$ and $R_w = 0.045$ for **1a**; $R = 0.044$ and $R_w = 0.042$ for **3**.

Selected atomic coordinates and equivalent isotropic temperatures factors for complexes **1a** and **3** are listed in Tables 5 and 6, respectively.

Tables of anisotropic temperature factors, hydrogen fractional coordinates and isotropic temperature factors and structure factors are available from the authors.

Acknowledgements

We thank Instituto Nacional de Investigação Científica for finantial support and Junta Nacional de Investigação Científica e Tecnológica for a research grant to V. Félix.

Appendix

All the calculations were of the extended Hückel type [21] with modified H_{ij}'s [27]. The basis set for the molybdenum atom consisted of 5*s*, 5*p* and 4*d* orbitals while for phosphorus, tin and chlorine only *ns* and *np* orbitals were used. The *s* and *p* orbitals were described by single Slater type wave functions and *d* orbitals were taken as contracted linear combinations of two Slater type wave functions. Standard parameters were used for C and N, while those for molybdenum, tin and chlorine are given in Table 7.

The geometry of the model compound, $[Mo(Cp)_2H(PH_3)]^+$ was taken from that for $[Mo(Cp)_2H(PPh_3)]^+$ [16] and for $[Mo(Cp)_2H(SnCl_3)]$ the experimental values [16] were used. The distances (Å) and angles (°) adopted were: Mo–Cp 2.00,

Table 7

Orbitals and parameters for the Extended Hückel calculations

Orbital	$-H_{ii}$/eV	ζ_1	ζ_2	C_1	C_2
Mo 5*s*	8.77	1.96			
Mo 5*p*	5.60	1.90			
Mo 4*d*	11.06	4.54	1.90	0.5899	0.5899
P 3*s*	18.60	1.60			
P 3*p*	14.00	1.60			
Cl 3*s*	30.00	2.033			
Cl 3*p*	15.00	2.033			
Sn 5*s*	16.16	2.12			
Sn 5*p*	8.32	1.82			

C–C(Cp) 1.40, C–H 1.08, Mo–H 1.70, Mo–P 2.44, P–H 1.42, Mo–Sn 2.70, Sn–Cl 2.38, Cp–Mo–Cp 142, and P(Sn)–Mo–H 79.2 or as described in the text.

References

1 R. Bohra, P.B. Hitchcock, M.F. Lappert and W.-P. Leung, Polyhedron, 8 (1989) 1884.
2 A.N. Protsky, B.M. Bulychev, G.L. Soloveichik and V.K. Belsky, Inorg. Chim. Acta, 115 (1986) 121.
3 C.G. Azevedo, A.R. Dias, A.M. Martins and C.C. Romão, J. Organomet. Chem., 368 (1987) 57.
4 G.L. Geoffroy and M.G. Bradley, Inorg. Chem., 17 (1978) 2410.
5 F.W.S. Benfield, N.J. Cooper, and M.L.H. Green, J. Organomet. Chem., 7 (1974) 49.
6 M.G. Harriss, M.L.H. Green and W.E. Lindsell, J. Chem. Soc. A, (1969) 1453.
7 J. Okuda, PhD Dissertation, Technische Hochschule Aachen, 1984.
8 J.W. Lauher and R. Hoffmann, J. Am. Chem. Soc., 98 (1976) 1729.
9 M.J. Calhorda, M.A.A.F. de C.T. Carrondo, R. Gomes da Costa, A.R. Dias, M.T.L.S. Duarte and M.B. Hursthouse, J. Organomet. Chem., 320 (1987) 53.
10 E. Cannilo, A. Coda, K. Prout and J.C. Daran, Acta Cryst. B, 33 (1977) 2608.
11 C.G. Azevedo, M.A.A.F. de C.T. Carrondo, M.F.M.M.M. Piedade and C.C. Romão, Z. Krist., 185 (1989) 365.
12 M.M. Kubicki, R. Kergoat, M. Curiou and P. L'Haridon, J. Organomet. Chem., 322 (1987) 357.
13 J.J. Daly, J. Chem. Soc., (1964) 3799.
14 A.J. Schultz, K.L. Stearley, J.M. Williams and R. Mink, Inorg. Chem., 16 (1977) 3303.
15 M.A.A.F. de C.T. Carrondo, A.R. Dias, A.M.T.S. Domingos and A.M. Galvão, Communication presented in X Encontro da Sociedade Portuguesa de Química, 1987.
16 A. Gusev, N.I. Kirillova, A.N. Protsky, B.M. Bulychev and G.L. Soloveichik, Polyhedron, 3 (1984) 765.
17 M.M. Kubicki, R. Kergoat, L.G. Lima, M. Cariou, H. Scordia and J.E. Guerchais, Inorg. Chim. Acta, 104 (1985) 191.
18 M.J. Calhorda, M.A.A.F. de C.T. Carrondo, M.H. Garcia and M.B. Hursthouse, J. Organomet. Chem., 342 (1988) 209.
19 T.S. Cameron and C.K. Prout, J. Chem. Soc. Dalton, (1972) 1447.
20 K.W. Muir, J. Chem. Soc. A, (1971) 2663.
21 R. Hoffmann, J. Chem. Phys., 39 (1963) 1397; R. Hoffmann and W.N. Lipscomb, J. Chem. Phys., 36 (1962) 2179.
22 J.D.J. Backer-Dirks, Ph.D. Thesis, University of London, 1983.
23 M.J. Calhorda, M.A.A.F. de C.T. Carrondo, A.R. Dias, C.F. Frazão, M.B. Hursthouse, J.A. Martinho Simões and C. Teixeira, Inorg. Chem., 27 (1988) 2513.
24 G.M. Sheldrick, SHELX Crystallographic Calculations Program, University of Cambridge, 1976.
25 C.K. Johnson, ORTEPII, Report ORNL-5138, Oak Ridge National Laboratory, Tennessee, 1976.
26 International Tables for X-Ray Crystallography, Vol. IV, Kynoch Press, Birmingham, England, 1974.
27 J.A. Ammeter, H.B. Bürgi, J.C. Thibeault and R. Hoffmann, J. Am. Chem. Soc., 100 (1978) 3686.